



Analysis of GNSS-R delay-Doppler maps from the UK-DMC satellite over the ocean

M. P. Clarizia,^{1,2} C. P. Gommenginger,¹ S. T. Gleason,¹ M. A. Srokosz,¹
C. Galdi,² and M. Di Bisceglie²

Received 9 October 2008; revised 10 December 2008; accepted 18 December 2008; published 29 January 2009.

[1] A study of the retrieval of sea surface roughness using Global Navigation Satellite System-Reflectometry (GNSS-R) from satellite is presented. Delay-Doppler Maps (DDMs) from the SSTL UK-DMC satellite are analyzed to retrieve directional Mean Square Slopes (MSSs). Results are compared to theoretically-derived MSSs and in situ measurements from co-located buoys of the National Data Buoy Center (NDBC), showing good agreement in most cases. Here, the whole DDM, a more complete source of information, is exploited for the first time using satellite GNSS-R data. These are potentially able to provide high spatial and temporal sampling, and therefore offer an improved way to observe wind and waves by means of a very modest instrument. **Citation:** Clarizia, M. P., C. P. Gommenginger, S. T. Gleason, M. A. Srokosz, C. Galdi, and M. Di Bisceglie (2009), Analysis of GNSS-R delay-Doppler maps from the UK-DMC satellite over the ocean, *Geophys. Res. Lett.*, 36, L02608, doi:10.1029/2008GL036292.

1. Introduction

[2] It has been widely demonstrated that signals emitted from Global Navigation Satellite System (GNSS) constellations (GPS, GLONASS, and Galileo) can be used not only for positioning, but also for remote sensing. In particular, GNSS signals scattered by the surface of the ocean carry information about the sea surface, and can be exploited to investigate its geophysical properties. This technique, first proposed by *Martin-Neira* [1993], and now known as GNSS-Reflectometry (GNSS-R), represents an innovative approach to ocean remote sensing. *Ruffini et al.* [2003] pointed out that GNSS-R for oceanography primarily aims at investigating three important geophysical parameters, namely directional Mean Square Slope (MSS), Significant Wave Height (SWH) and Mean Sea Level (MSL). Consequently, GNSS-R has both scatterometric (sea roughness, wind speed and direction) and altimetric (SWH and MSL) applications. Excellent temporal sampling, global coverage, and long-term GNSS mission lifetimes are among the factors of GNSS signals which make this technique very attractive, and particularly suitable for observing the ocean surface, which is highly variable in space and time. Our analysis focuses on the investigation of sea surface roughness using satellite-measured GPS-Reflected signals from the Surrey Satellite Technology Ltd UK-DMC mission, which are the only satellite GNSS-R data available to-date.

From these data, we have retrieved MSS in two orthogonal directions and the principal wave slope direction, using a 2D representation of the scattered GPS signal power as a function of the time delay and the Doppler frequency, the so-called Delay-Doppler Map (DDM). To-date, researchers have analyzed 1D delay waveforms from data collected during airborne campaigns [e.g., *Garrison et al.*, 1998; *Cardellach et al.*, 2003] or from the UK-DMC satellite [*Gleason et al.*, 2005], to derive total mean square slope or sea surface wind speeds. The advantages of using 2D DDMs were highlighted by *Germain et al.* [2004], who inferred directional MSS using DDMs from data collected during an airborne campaign. In our case, we benefit from the twofold advantage of using DDMs and satellite data, which in principle are globally distributed and constantly available and accessible, without the need to fly ad-hoc campaigns. The GNSS-R technique is based upon a bistatic configuration of the transmitter and receiver, and the scattering problem involves L-Band (1.2–1.5 GHz) GPS signals transmitted from satellites at altitudes of about 20000 km, which are scattered off the ocean and received onboard the low-orbit sun-synchronous UK-DMC satellite, at an altitude of about 680 km. The main contribution to the scattered signal power at the receiver comes from the Specular Point (SP) on the surface, and an area around it called the Glistening Zone (GZ), which widens with increasing sea surface roughness. The scattering of GNSS signals can be described using Geometric Optics (GO), according to which it depends mainly on the Probability Density Function (PDF) of the large scale surface slopes. If we assume the statistics of the waves are Gaussian, a reasonable assumption, the PDF is entirely characterized by three variables: two MSSs along the major and minor axes of the 2D Gaussian PDF, and an angle which defines the rotation of the principal axis with respect to true north, and therefore identifies the principal scattering direction, to within a 180° ambiguity. We retrieved these geophysical parameters by comparing UK-DMC DDMs with theoretical DDMs from a GO model. Details of the DDM processing are given in section 2. Section 3 explains the retrieval of the directional MSSs and the principal and secondary surface slope directions. In section 4, results are compared with theoretical MSS estimates as well as with collocated in situ data from buoys of the National Data Buoy Center (NDBC). Finally, section 5 states the conclusions.

2. UK-DMC Data Processing

[3] The data were collected onboard UK-DMC, equipped with a GPS receiver, a solid state data recorder and a Left-Hand Circularly Polarized (LHCP) medium gain antenna

¹National Oceanography Centre Southampton, Southampton, UK.

²Università degli Studi del Sannio, Benevento, Italy.

Table 1. Available UK-DMC GPS-R Data Collections, Together With Collocated in Situ Measurements by NDBC Buoys^a

Label	Date/Time	Region	NDBC Buoy Id	Buoy WS (m/s)	Buoy WD (deg)	Buoy MWD (deg)	Buoy SWH (m)	SCR (km)
R12	16/11/04 07:54	NW Pacific	46006	8.3	253	N/A	2.80	[38–56]
R20	21/03/05 07:29	NW Pacific	46002	3.6	297	N/A	4.30	[32–58]
R21	02/05/05 09:16	Hawaii	51001	4.5	23	N/A	1.98	[1–44]
R29	29/10/05 14:40	Virginia	44014	9.4	326	341	1.68	[70–79]

^aWS is wind speed, WD is wind direction, MWD is mean wave direction, and SCR is space collocation range, given by the distance of the buoy from the closest to farthest SP within the 12-second time interval. The buoy directions are measured clockwise with respect to true north.

(peak gain of 11.8 dBiC) pointing downward, and covering a large footprint (3 dB beam of about 1000 km × 200 km). The Daaxa GPS software receiver we used to process the data on-ground, illustrated by Gleason [2006], performs a down conversion of the signal to base band, and samples it at a rate of 5.714 MHz. Subsequently, the signal is coherently correlated with a locally generated C/A code replica to produce a single “look”, and multiple looks are then incoherently summed to produce the final delay-Doppler map. DDMs are computed using a delay step of 0.18 C/A code chip (1 chip ~ 1 μs), and a Doppler bin of 100 Hz. The choice of the Doppler bin represents a trade-off between the need to reduce noise and the need to maintain a good resolution and hence preserve features in the map. We coherently integrated 1 ms of data, following Gleason [2006], where the maximum correlation power is obtained for a coherent integration time close to 1 ms. This result is linked to the length of the C/A code (which is about 1 ms), as well as to the changing scattering geometry due to the satellite motion, which limits the coherence of the received signal. The incoherent accumulation time was chosen equal to 1 second and 12 seconds respectively. The choice of the 1-second accumulation time is consistent with the averaging used in satellite nadir altimetry. Moreover, it represents a convenient choice, as it allows us to estimate the variability of the parameters within a 12-second time interval. The choice of the 12-second accumulation time helps increase the signal-to noise ratio in the DDM. This gives a smoother DDM, which is easier to fit, but provides no insight into the variability of the retrieved parameters. It is worth noting that during the accumulation time the signal experiences a shift both along the Doppler and (above all) along the delay axes, which must be accounted for when the single looks or the single maps are accumulated. During a 1 second accumulation time, the shift along the delay axis has been estimated for each millisecond, and used to align the consecutive looks before accumulating them. This shift is nearly linear over 1 second (the second derivative of the code delay can be neglected), whereas the shift along the Doppler direction is negligible. For the 12 second accumulation time, the shift along the Doppler direction also starts to play a role, and single 1-second DDMs are aligned using the 2D cross-correlation between them. Here, the analysis was carried out on four data sets only, as they were the only data available at the time. These data were collected at different times, for different Pseudo Random Noise (PRN) codes (which identify the GPS satellites) and different sea conditions. All were collocated with in situ measurements of wind and waves by NDBC buoys to within 1 hour and 100 km [Gommenginger et al., 2002]. Table 1 shows the co-located buoy data for wind speed, wind direction, and Significant Wave Height (SWH), for each data collection. An examination of the buoy wind/wave histories (not shown) indi-

cates that the four situations are atypical seas. The wind/wave history for dataset R12 indicates a moderate but highly variable wind speed with a lot of swell, whereas R20 corresponds to a decaying sea with rapidly decaying wind speed (from 12 m/s to 4 m/s in 12 hours). For R21, the buoy history shows overall steady wind conditions of around 5 m/s wind speed, with some swell, while R29 corresponds to conditions of growing sea.

3. Simulated Delay-Doppler Maps

[4] Once DDMs from satellite data have been generated, we estimate the parameters of interest by comparing them with simulated DDMs. The GO model used was developed by Zavorotny and Voronovich [2000] and describes the scattering of GNSS signals from the sea surface. The average GPS scattered power, as a function of delay and Doppler frequency, is:

$$\langle P_s(\tau, f) \rangle \propto \iint \frac{G_R(r)}{R_T^2(r)R_R^2(r)} \frac{q^4(r)}{q_z^4(r)} P\left(\frac{-q_x(r)}{q_z(r)}\right) \cdot \chi^2[\tau - \tau_k(r), f - f_k(r)] dr \quad (1)$$

where r represents the spatial coordinate on the scattering surface, $G_R(r)$ is the receiver antenna gain, $R_T(r)$ and $R_R(r)$ are the ranges between the scattering point and the transmitter and receiver respectively, $\chi[\tau - \tau_k(r), f - f_k(r)]$ is the Woodward Ambiguity Function (WAF) of pseudorandom GPS sequences, function of the delay and Doppler coordinates $\tau_k(r)$ and $f_k(r)$, $q(r) = [q_x(r), q_y(r), q_z(r)]$ is the scattering vector, and finally $P(-q_x(r)/q_z(r), -q_y(r)/q_z(r))$ is the sea surface slope PDF, assumed to be a two-dimensional zero-mean Gaussian distribution. The PDF is characterized by two MSSs along the major and minor axes of the PDF ellipse, and by a rotation angle Φ of the major axis of the PDF (which we take as the principal scattering direction) with respect to true north. However, we emphasize that a 180° ambiguity characterizes the rotation angle due to the symmetry of the PDF. The DDM simulation requires the calculation of the SP, as well as some geometrical conversions, for which the satellite positions and velocities are needed. We have used the actual positions and velocities of GPS satellites and UK-DMC to generate DDMs and fit them to the 1-second measured DDMs. For the fitting to 12-second averaged DDMs, we averaged positions and velocities over a 12-second interval to generate the simulated DDM. An example of a 1-second DDM from UK-DMC data (top), and a modelled DDM (bottom) is shown in Figure 1. This shows similarities in the overall horseshoe shape of the two maps, but the real DDM exhibits some additional horizontal striping patterns, not present in the simulated map. Such patterns could be either linked to some residual speckle

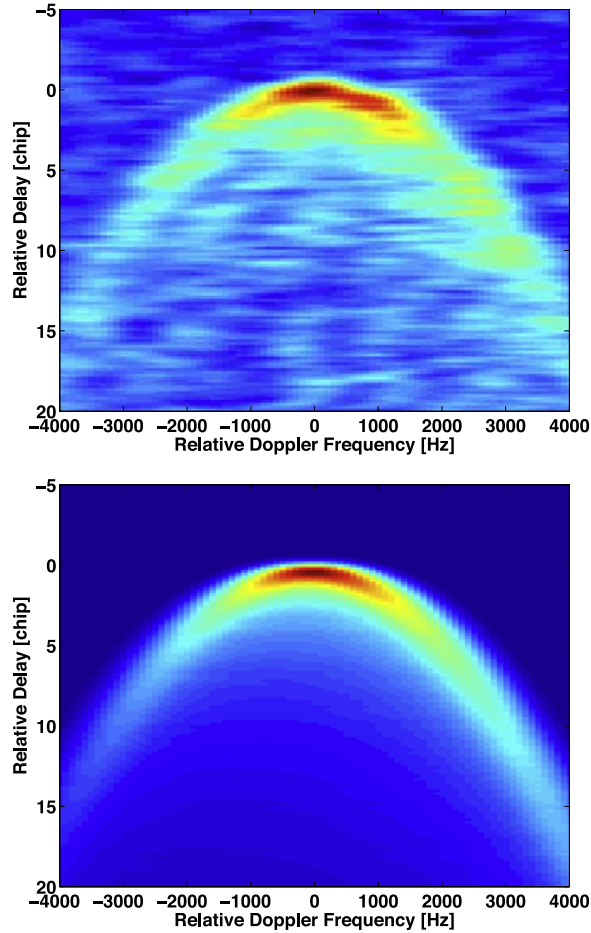


Figure 1. (top) Measured DDM obtained from the first second of UK-DMC R21 data and (bottom) simulated DDM using the Zavorotny-Voronovich model. Both delays and Doppler frequencies are expressed relative to those at the SP.

noise, or other types of scattering (i.e., Bragg scattering), not taken into account by the theoretical model. We have performed a least-square fit between measured and simulated DDM, to find the optimal PDF parameters, for the four data sets. However, we were not able to exploit the magnitude information in the DDMs, and only used the shape for the retrievals, due to the significant difference in the power values. This difference is primarily due to the lack of a calibration of the incident GPS signal, as well as unrecorded effects within the receiver (amplifiers, automatic gain control), affecting the amplitude of the received signals. We defined a scale parameter a and offset parameter b as further variables to be optimized, such that the new simulated DDM becomes $P_S'(\tau, f) = aP_S(\tau, f) + b$. A joint estimation of five variables (MSS_1 , MSS_2 , Φ , a , b) was performed to minimize the residual error between UK-DMC and modelled DDM, with a standard non linear least-square minimization routine using MATLAB.

4. Results and Discussion

[5] Figure 2a shows the median of 12 retrieved total MSS from 12 1-second DDMs. The variability is represented with the Median Absolute Value (MAD), defined as the median

of the absolute residuals from the median of the data. The choice of more robust statistics to represent the results was dictated by the presence of outliers in the retrievals, possibly caused by convergence of the fitting algorithm to local minima in some cases. The total MSS is simply calculated here as the sum of the two MSSs along the major and minor axes of the PDF ellipse. Figure 2a also shows the single retrieved total MSS from the 12-second average DDM. All results are plotted versus the buoy wind speed for each data collection. Unlike *Germain et al.* [2004], we could not compare our results with altimeter-derived MSSs, as no suitable altimeter data was available within acceptable

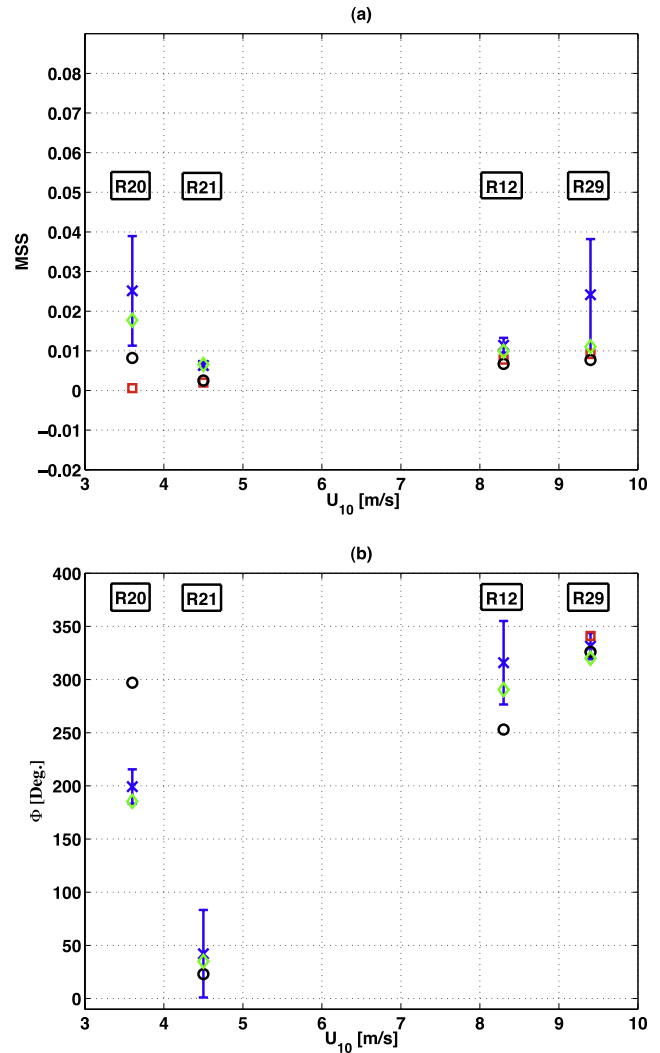


Figure 2. (a) Median of the total retrieved MSSs from 1-second DDMs over 12 seconds (crosses) with MAD (as error bars) and MSSs estimated from 12-second averaged DDM (diamonds), versus buoy wind speed. Total MSSs from the truncated theoretical Elfouhaily wind wave spectrum (squares) and buoy-derived total MSSs (circles) are also illustrated for comparison. (b) Median of the retrieved principal slope directions from 1-second DDMs (crosses) with MAD (error bars) and slope directions estimated from 12-second averaged DDM (diamonds), versus buoy wind speed. Buoy wind directions (circles) and MWD (square) are given for comparison.

space/time separation limits. From Figure 2a, we notice the good agreement and lower variability for the case of R21 (steady conditions with some swell) and R12 (swell, high wind speed variability), compared to the cases of R20 (decaying sea) and R29 (growing sea), where the median MSSs are higher than the buoy measurements. This could be explained for R29 by the stronger wind speed, generating higher short waves, not sensed by the buoys, which would raise the MSS retrieved from the GPS-R signals. The wind/wave conditions for R20 are more subtle, in that the wind speed was quite high (12 m/s) before the acquisition time, and rapidly dropped to 4 m/s at the time the data were collected, possibly leaving behind a wind wave component and therefore a higher MSS, not related to the instantaneous wind speed. In Figure 2a, our estimated MSSs are compared with MSSs calculated by integrating the buoy measured wave spectrum, which covers a range of wavelengths down to 9.75 m only, and by integrating the theoretical Elfouhaily *et al.* [1997] wind wave spectrum, down to a specific wavelength cutoff, which was again set to 9.75 m. The Elfouhaily spectrum is theoretically derived under the assumption of well-developed wind seas, whereas the buoy spectrum is obtained from real measurements.

[6] Figure 2a highlights that our retrieved MSSs show the same behaviour as the buoy-measured MSSs, and are always higher than them, which is consistent with the sensitivity of the GPS wavelength (19 cm) to shorter waves. For MSSs retrieved from single second DDMs, we get good results for the cases of R21 and R12, as the MAD is quite small, and both the buoy and the theoretical Elfouhaily-truncated MSSs are in good agreement with our estimates. Very good results are obtained for MSSs retrieved from averaged 12-s DDMs, as they appear to be quite close to both the values measured by the buoys and the MSSs obtained from the theoretical spectrum, except at R20 (rapidly decaying sea). The retrieved principal surface slope direction results are plotted in Figure 2b versus buoy wind speed. The Mean Wave Direction (MWD) was available only for R29, when wind and wave directions were aligned. As illustrated in Figure 2b, the overall behaviour of the retrieved directions follows that of the buoy wind directions. We find good agreement between our 12-second median principal direction from 12 1-second DDMs and the buoy measurements for R21 and R29. However, we recall that a 180° ambiguity affects our direction retrieval. As compared to MSS, this time we have a complementary behaviour, as we find a higher variability in the retrieved direction for the cases of R21 and R12, and a lower variability for the cases of R20 and R29. Indeed, the PDFs for R20 and R29 are more anisotropic (i.e., the ratio between the retrieved secondary and principal MSS is smaller on average compared to the other two cases), and thus they exhibit a predominant slope direction which is retrieved with less ambiguity. Our retrieved slope directions from averaged 12-s DDMs are also in very good agreement with the buoy measurements, and we notice that the worst match is obtained for R20, as in the case of the MSS.

5. Conclusions

[7] We have analyzed GPS-Reflected DDMs from spaceborne altitudes from four UK-DMC data acquisitions and

extracted the directional MSS and principal wave slope direction by least-square fitting a theoretical DDM. Our retrieved values are generally consistent with the buoy measurements. The retrieved median MSSs and direction from 1-second DDMs are consistent with both theoretical values and in situ measurements for the four cases. In particular, we obtained good agreement for the median MSS for steady wind and wave conditions with some swell (R21) and for swell with high wind speed variability (R12), and for the median slope direction for R21 and for growing sea conditions (R29). The retrieved MSSs from averaged 12-s DDM are close to the buoy measurements for both MSSs and slope directions, except for the case of decaying sea, with rapidly decaying wind speed (R20). Our analysis of satellite DDMs complements previous analyses of satellite delay waveforms and DDMs from aircraft campaigns. Notably, the exploitation of DDMs allows us to retrieve not only roughness, but also surface slope direction. The results obtained therefore offer convincing evidence for using GNSS-R to retrieve wind and wave data using a small passive instrument that could easily be fitted on more satellites. Our study also highlights marked differences between measured and simulated DDMs which could be linked to either the instrumentation and processing, or geophysical processes not accounted for in the GO-based model. In the latter case, a way forward could be to simulate the whole end-to end scattering problem for an explicit ocean surface, accounting for all the relevant scattering mechanisms. Also, with more UK-DMC data now available, further comparisons between simulated and measured DDMs could be performed for other sea conditions, which would help us understand better what ocean properties affect the GPS-R signals. Collocated data from Altimeters, Scatterometers or Synthetic Aperture Radars may also provide additional information on wind and wave conditions to extend the ground truth for the UK-DMC datasets. Finally, the 180° ambiguity in our direction retrievals could be eliminated, perhaps using the Doppler information, in order to identify how the principal surface slopes are oriented.

[8] **Acknowledgments.** We thank Martin Unwin from SSTL for helpful advice and access to the UK-DMC GPS-Reflectometry data under the Satellite Data Evaluation and Research Licence Agreement between SSTL and NOCS. Thanks also to Paolo Cipollini from NOCS for useful discussions.

References

- Cardellach, E., G. Ruffini, D. Pino, A. Rius, A. Komjathy, and J. Garrison (2003), Mediterranean Balloon Experiment: Ocean wind speed sensing from the stratosphere using GPS reflections, *Remote Sens. Environ.*, *88*, 351–362.
- Elfouhaily, T., B. Chapron, K. Katsaros, and D. Vandemark (1997), A unified directional spectrum for long and short wind-driven waves, *J. Geophys. Res.*, *102*, 15,781–15,796.
- Garrison, J. L., S. J. Katzberg, and M. I. Hill (1998), Effect of sea roughness on bistatically scattered range coded signals from the Global Positioning System, *Geophys. Res. Lett.*, *25*, 2257–2260.
- Germain, O., G. Ruffini, F. Soulat, M. Caparrini, B. Chapron, and P. Silvestrin (2004), The Eddy Experiment: GNSS-R speculometry for directional sea-roughness retrieval from low altitude aircraft, *Geophys. Res. Lett.*, *31*, L12306, doi:10.1029/2004GL019994.
- Gleason, S. T. (2006), Remote sensing of ocean, ice and land surfaces using bistatically scattered GNSS signals from low Earth orbit, Ph.D. thesis, Univ. of Surrey, Surrey, U.K.
- Gleason, S. T., S. Hodgart, S. Yiping, C. P. Gommenginger, S. Mackin, M. Adjrjad, and M. Unwin (2005), Detection and processing of bistatically

- reflected GPS signals from low Earth orbit for the purpose of ocean remote sensing, *IEEE Trans. Geosci. Remote Sens.*, *43*, 1229–1241.
- Gommenginger, C. P., M. A. Srokosz, P. G. Challenor, and P. D. Cotton (2002), Development and validation of altimeter wind speed algorithms using an extended collocated buoy/TOPEX data set, *IEEE Trans. Geosci. Remote Sens.*, *40*, 251–260.
- Martin-Neira, M. (1993), A Passive Reflectometry and Interferometry System (PARIS): Application to ocean altimetry, *ESA J.*, *17*, 331–355.
- Ruffini, G., O. Germain, F. Soulat, M. Taani, and M. Caparrini (2003), GNSS-R: Operational applications, paper presented at Workshop on Oceanography with GNSS-R Reflections, Barcelona, Spain.
- Zavorotny, V. U., and A. G. Voronovich (2000), Scattering of GPS signals from the ocean with wind remote sensing application, *IEEE Trans. Geosci. Remote Sens.*, *38*, 951–964.
-
- M. P. Clarizia, S. T. Gleason, C. P. Gommenginger, and M. A. Srokosz, National Oceanography Centre Southampton, European Way, Southampton SO14 3ZH, UK. (marari@noc.soton.ac.uk)
- M. Di Bisceglie and C. Galdi, Università degli Studi del Sannio, Piazza Roma 21, I-82100 Benevento, Italy.